Lipid nanoparticle-targeted mRNA therapy as a treatment for the inherited metabolic liver disorder arginase deficiency

Brian Truong[a,b], Gabriella Allegri[c], Xiao-Bo Liu[b], Kristine E. Burke[d], Xuling Zhu[d], Stephen D. Cederbaum[e,f,g], Johannes Häberle[c], Paolo G. V. Martini[d], and Gerald S. Lipshutz[a,b,e,f,g,1]

[a]Department of Molecular and Medical Pharmacology, David Geffen School of Medicine at UCLA, Los Angeles, CA 90095; [b]Department of Surgery, David Geffen School of Medicine at UCLA, Los Angeles, CA 90095; [c]Division of Metabolism and Children's Research Center, University Children's Hospital, 8032 Zurich, Switzerland; [d]Moderna, Inc., Cambridge, MA 02139; [e]Department of Psychiatry, David Geffen School of Medicine at UCLA, Los Angeles, CA 90095; [f]Intellectual and Developmental Disabilities Research Center at UCLA, David Geffen School of Medicine at UCLA, Los Angeles, CA 90095; and [g]Semel Institute for Neuroscience, David Geffen School of Medicine at UCLA, Los Angeles, CA 90095

Edited by Dwight Koeberl, Duke University, Durham, NC, and accepted by Editorial Board Member David J. Mangelsdorf August 9, 2019 (received for review April 10, 2019)

Arginase deficiency is caused by biallelic mutations in arginase 1 (ARG1), the final step of the urea cycle, and results biochemically in hyperargininemia and the presence of guanidino compounds, while it is clinically notable for developmental delays, spastic diplegia, psychomotor function loss, and (uncommonly) death. There is currently no completely effective medical treatment available. While preclinical strategies have been demonstrated, disadvantages with viral-based episomal-expressing gene therapy vectors include the risk of insertional mutagenesis and limited efficacy due to hepatocellular division. Recent advances in messenger RNA (mRNA) codon optimization, synthesis, and encapsulation within biodegradable liver-targeted lipid nanoparticles (LNPs) have potentially enabled a new generation of safer, albeit temporary, treatments to restore liver metabolic function in patients with urea cycle disorders, including ARG1 deficiency. In this study, we applied such technologies to successfully treat an ARG1-deficient murine model. Mice were administered LNPs encapsulating human codon-optimized *ARG1* mRNA every 3 d. Mice demonstrated 100% survival with no signs of hyperammonemia or weight loss to beyond 11 wk, compared with controls that perished by day 22. Plasma ammonia, arginine, and glutamine demonstrated good control without elevation of guanidinoacetic acid, a guanidino compound. Evidence of urea cycle activity restoration was demonstrated by the ability to fully metabolize an ammonium challenge and by achieving near-normal ureagenesis; liver arginase activity achieved 54% of wild type. Biochemical and microscopic data showed no evidence of hepatotoxicity. These results suggest that delivery of *ARG1* mRNA by liver-targeted nanoparticles may be a viable gene-based therapeutic for the treatment of arginase deficiency.

arginase deficiency | hyperargininemia | lipid nanoparticle | mRNA | ureagenesis

Arginase deficiency (Online Mendelian Inheritance in Man phenotype [OMIM]:207800) is an uncommon autosomal recessive disorder [estimated incidence of 1:950,000 in the United States (1)] that results from loss of arginase 1 (ARG1) (Enzyme Commission 3.5.3.1). ARG1 is the final enzyme of the urea cycle completing the major metabolic pathway for the disposal of excess nitrogen in terrestrial mammals. Along with red blood cells, the cytosolic enzyme is most prevalent in hepatocytes hydrolyzing arginine into ornithine, which then reenters the cycle, while nitrogen, in the form of urea, is excreted as waste in the urine (2).

The typical presentation of arginase deficiency is different from that of the other urea cycle disorders (UCDs), with the onset of symptoms typically in late infancy. Outcomes include microcephaly, seizures, loss of ambulation, clonus, spastic diplegia, intellectual disability (from mild to severe), growth deficiency, and failure to thrive (3, 4); the exact cause of these neurological manifestations and the progressive intellectual decline are not known but are hypothesized to be related to hyperargininemia and the accumulation of guanidino compounds (as putative neurotoxins) found in the plasma, urine, and cerebrospinal fluid of these patients (5–10). Unlike the other enzyme deficiencies of the urea cycle, hyperammonemia is uncommon (11), and thus patients typically avoid the severe nitrogen vulnerability and catastrophic crises that occur in the other UCDs. However, the neurological decline is progressive and unrelenting, and the mainstay of current-day therapy, which includes provision of a very strict protein-restricted diet, amino acid supplementation, and administration of the nitrogen scavengers sodium benzoate and sodium phenylbutyrate (3, 4), only partially alleviates the disorder, as there exists no medical therapy that is completely efficacious. While liver transplantation has not been commonly employed for patients with this disorder, long-term follow-up of 2 patients who underwent liver transplantation showed normalization of plasma arginine and guanidino compounds with lack of progressive neurological decline (12, 13), further supporting

Significance

Systemically administered lipid nanoparticles (LNPs) targeting the liver were able to express the cytoplasmic enzyme arginase 1 (ARG1) in a conditional knockout model of ARG1 deficiency. Metabolically, this resulted in maintaining normal plasma ammonia and arginine, preventing the build-up of excessive hepatic arginine, and obviated the development of guanidino compounds, a hallmark of this enzyme deficiency. Unlike controls, repeat dosing of LNPs encapsulating human codon-optimized *ARG1* messenger RNA led to long-term survival without evidence of toxicity, restoration of ureagenesis, and the ability to handle toxic ammonia loading. These findings have implications for therapy of ARG1 deficiency, which is presently inadequately treated and leads to progressive neurological decline.

Author contributions: B.T. and G.S.L. designed research; B.T., G.A., X.-B.L., K.E.B., X.Z., and G.S.L. performed research; J.H. and P.G.V.M. contributed new reagents/analytic tools; B.T., X.-B.L., S.D.C., J.H., P.G.V.M., and G.S.L. analyzed data; and B.T. and G.S.L. wrote the paper.

Conflict of interest statement: G.S.L. has served as a consultant to Audentes Therapeutics in an area unrelated to this work. S.D.C. is a consultant for Synlogic and Cobalt Biomedicine in areas unrelated to this work. K.E.B., X.Z., and P.G.V.M. are current or previous employees of Moderna, Inc. and receive salary and stock options as compensation for their employment.

This article is a PNAS Direct Submission. D.K. is a guest editor invited by the Editorial Board.

See Commentary on page 20804.

[1]To whom correspondence may be addressed. Email: glipshutz@mednet.ucla.edu.

This article contains supporting information online at www.pnas.org/lookup/suppl/doi:10.1073/pnas.1906182116/-/DCSupplemental.

First published September 9, 2019.

methods of normalization of plasma arginine levels as tenets of therapy.

With the development of transgenic technology and the advances of the last 2.5 decades in the progress and application of gene therapy to monogenic disorders of the liver, our group has been successful in the development of a mouse model of hyperargininemia (14), along with the preclinical application of viral-based gene therapy approaches in treating this enzyme deficiency (15–17). The beginning of therapy before (18, 19) or shortly after (20, 21) birth, before the onset of phenotypic disease, has advantages, as early gene therapy has the potential to ameliorate genetic abnormalities before the development of phenotypic disease. For example, initiating therapy shortly after birth has demonstrated that both restoring hepatic arginase activity and controlling hyperargininemia and guanidino compounds lead to normal neurological development, cognitive activity, and behavior in Arg1-deficient mice (22, 23).

However, such therapy with episomal viral vectors [as adeno-associated virus (AAV) typically only integrates at a low frequency (24)] is faced with greater challenges in rapidly dividing tissues and organs than therapy of postmitotic tissues (25). In neonates, the rate of hepatocellular proliferation is much higher and affects the maintenance of episomal vector genomes (26, 27), while rapid cellular proliferation in adults is uncommon. For example, individual hepatocytes in the adult mouse liver are replaced once every 180 to 400 d (28, 29), while the neonatal murine liver increases from 50 mg to over 1 gram in the first 5 postnatal weeks (25). When administered to neonatal mice, this results in a decline in AAV copy number of over 3 logs (25) leaving relatively few arginase-expressing hepatocytes over the long term in adult animals and the potential for nitrogen vulnerability (16, 17). While enzyme replacement has led to successful therapies for a number of other genetic disorders, when tested in arginase-deficient mice, plasma arginine was reduced (11); however, repeat dosing did not result in improved survival or prevention of weight loss, likely due to the inability of the PEGylated enzyme to enter hepatocytes. Thus, today, there remains an unmet need for these patients.

Messenger RNA (mRNA) therapy with nanoparticle encapsulation for systemic delivery to hepatocytes has the potential to restore metabolic enzymatic activity for a number of hepatic metabolic disorders (30, 31), including arginase deficiency. Until recently, RNA-based therapeutics have suffered from problems of poor translatability, lack of stability, immune responses, hepatotoxicity (32), and inefficient delivery (30, 33). Recent advances have improved the stability and translatability of RNAs and have made them immunologically inactive (30). While the advantages include avoidance of insertional mutagenesis and lack of constitutive gene activation, the use of mRNA technology may also allow for restoration of inaccessible targets (31), such as cytoplasmic arginase activity, which was unachievable with PEGylated enzymatic therapy (11).

In this study, we encapsulated and systemically administered human codon-optimized *ARG1* (h*ARG1*) mRNA to a conditional knockout murine model of ARG1 deficiency. We achieved delivery of mRNA to the liver by lipid nanoparticles (LNPs) at therapeutic levels in this preclinical model. We successfully demonstrated high-level hepatic arginase expression and function with restoration of ureagenesis, while achieving long-term survival, maintenance of weight, normalization of plasma ammonia and arginine, lack of hepatic guanidinoacetic acid (GAA; a guanidino compound), and normalization of hepatic arginine without evidence of hepatotoxicity. These findings demonstrate the efficacy of this approach in arginase deficiency.

Results

LNPs Successfully Deliver mRNA to Murine Livers. The liver is the primary location of nitrogen detoxification and urea cycle function. Therefore, targeted delivery of the LNPs and proper release of the encapsulated mRNA for therapeutic protein translation in the liver are crucial to the potential success of this treatment modality for arginase deficiency. To examine the ability of our engineered LNPs to traffic to the liver, we administered a single intravenous (IV) bolus of 2 mg/kg of LNP-encapsulated firefly (*Photinus pyralis*) luciferase mRNA (LNP-*luc*) to wild-type (WT) conditional arginase-deficient ($Arg1^{flox/flox}$) mice ($n = 5$ males). Beginning 2 h after LNP-*luc* injection, mice were administered the luciferase substrate D-Luciferin and underwent serial bioluminescent imaging (BLI). Imaging revealed proper localization of functional luciferase protein to the liver as early as 2 h after LNP-*luc* injection that remained detectable by BLI in some animals up to 36 h postinjection (Fig. 1*A*). At 72 h after the initial LNP-*luc* injection, luciferase protein was undetectable by BLI, and an additional IV bolus of 2 mg/kg of LNP-*luc* was administered at 73 h after the first injection. Repeat serial BLI revealed liver trafficking and luciferase protein translation and stability kinetics comparable to the initial LNP-*luc* injection (Fig. 1 *A* and *B*). Although the protein translation kinetics and half-life will be variable and determined by the specific mRNA encapsulated within the LNPs, BLI demonstrated the ability of LNPs to reliably and repeatedly deliver mRNA to the liver without overt evidence of short-term abnormalities.

Pharmacokinetic Characterization of LNP-Encapsulated Arginase mRNA in Murine Livers. The h*ARG1* mRNA was designed, synthesized, and encapsulated within our biodegradable liver-targeting LNPs (LNP-h*ARG1*). To characterize the kinetics of the h*ARG1* mRNA release from the LNPs and stability within the liver, we performed a pharmacokinetic (PK) study in WT $Arg1^{flox/flox}$ mice ($n = 3$ mice per time point). We administered a single IV bolus of 2 mg/kg of LNP-h*ARG1* and collected livers at the time points of 0, 2, 6, 12, and 24 h and then daily from days 2 to 7 postinjection. Using quantitative real-time-PCR (qRT-PCR) primers specific for the h*ARG1* mRNA encapsulated within the LNPs, h*ARG1* mRNA levels in treated livers were determined relative to murine *Gapdh* housekeeping transcript levels. We observed peak and substantial h*ARG1* mRNA levels in the liver at the earliest time point 2 h postinjection compared with 0-h mice that did not receive LNP-h*ARG1* (0 h: 0.934 ± 9.934 vs. 2 h: $1.49 \times 10^5 \pm 2.06 \times 10^4$ relative transcript levels; $P < 0.001$) (Fig. 1*C*). After the observed peak at 2 h, h*ARG1* mRNA levels significantly decreased by 33.1% by 6 h ($P = 0.005$) and 84.2% by 12 h ($P < 0.001$) relative to 2-h postinjection mRNA levels. By 24 h, only 4.4% of the 2-h postinjection mRNA levels remained ($P < 0.001$), and levels were maintained below 0.25% from days 2 to 7 ($P < 0.001$ each day).

Long-Term Animal Survival after Systemic Delivery of LNP-h*ARG1*. Hepatic loss of murine Arg1 expression leads to hyperargininemia, hyperammonemia, and death in $Arg1^{-/-}$ mice (34). Previous studies have demonstrated that delivery of the murine Arg1 complementary DNA (cDNA) by AAVrh10 can rescue a juvenile-lethal arginase-deficient murine model, whose therapeutic efficacy may be limited due to hepatocellular division, leading to eventual dilution and a substantial reduction of the transgene expression (16). To demonstrate the long-term efficacy of LNP-mediated delivery of codon-optimized h*ARG1* mRNA to successfully treat arginase deficiency, adult $Arg1^{flox/flox}$ mice were administered 2.0×10^{11} genome copies of AAV8-thyroxine binding globulin promoter (TBG)-Cre recombinase (Cre) on day 0 to disrupt hepatic expression of the endogenous functional murine Arg1 by excision of exons 7 and 8. Beginning on day 14 after AAV8-TBG-Cre administration, mice were administered IV either 2 mg/kg of LNP-*luc* or LNP-h*ARG1* ($n = 10$, 5 males and 5 females per group). One group was administered LNP-mRNA weekly, and another group was administered LNP-mRNA every 3 d (q3D). Weight was recorded daily, blood was collected weekly, and livers were collected at the end of the study or at the time of euthanasia

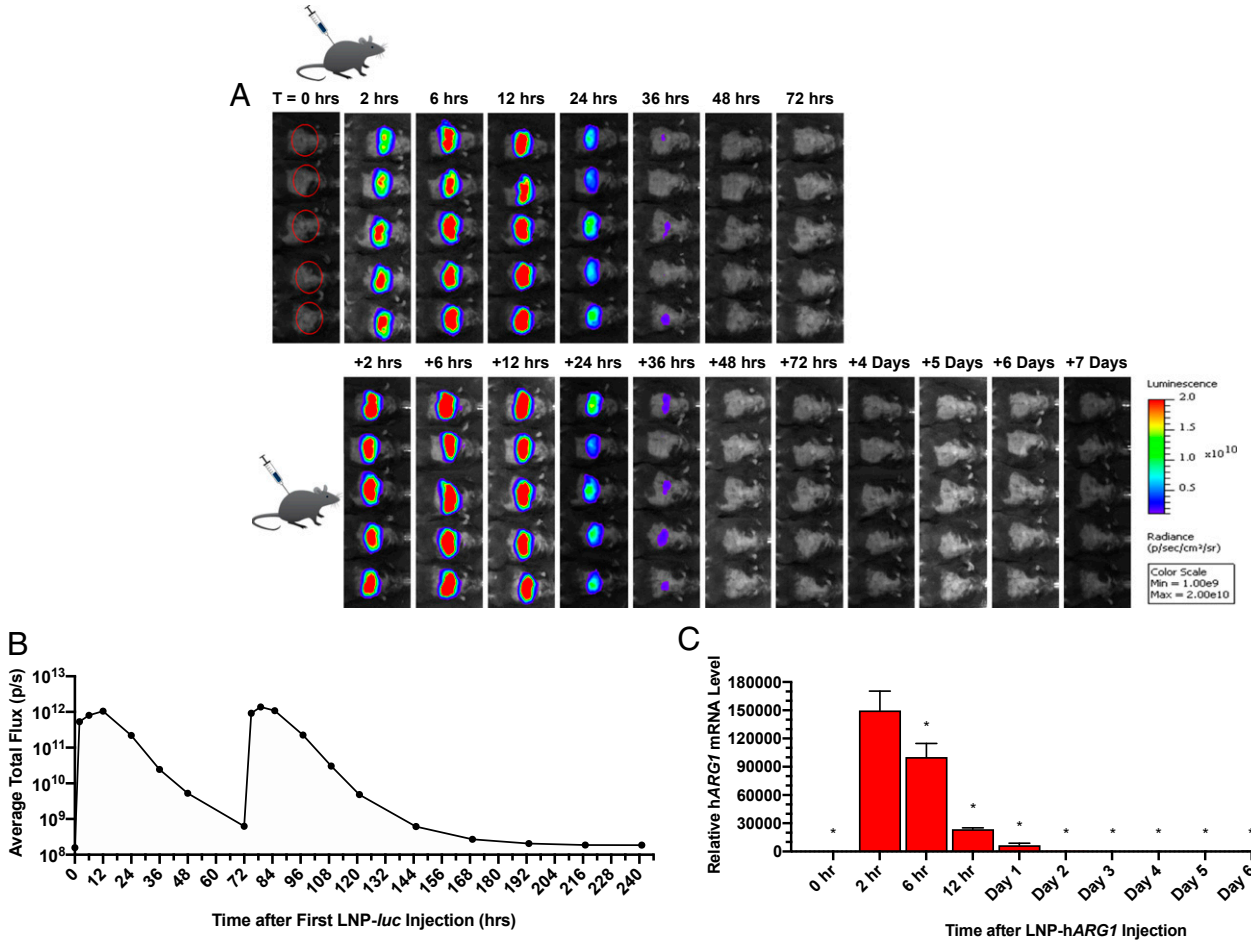

Fig. 1. LNP-mediated mRNA delivery to the liver results in repeatable hepatic expression. WT conditional Arg1 knockout mice were administered an IV bolus dose of 2 mg/kg of LNP-*luc* or LNP-h*ARG1*. (*A*) BLI of hepatic luciferase expression represented by a pseudocolor scale was performed at various time (T) points (0, 2, 6, 12, 24, 36, 48, and 72 h) after the first LNP-*luc* dose, with repeat imaging after the second bolus administration (2, 6, 12, 24, 36, 48, and 72 h; 4, 5, 6, and 7 d; $n = 5$ mice per time point). All images were acquired and processed with the same settings. Max, maximum; Min, minimum; p, photons; sr, steradian. (*B*) Quantitation of hepatic expression of firefly luciferase was performed after the initial LNP-*luc* bolus injection and after repeat administration. (*C*) PK characterization of h*ARG1* mRNA in the liver was determined by qRT-PCR after liver collection at various time points (0, 2, 6, 12, 24 h; 2, 3, 4, 5, 6, and 7 d; $n = 3$ per time point). *P* values were obtained from 1-way ANOVA with Tukey's multiple comparison test. *$P < 0.001$ compared with 2-h postinjection h*ARG1* mRNA levels. Data are presented as mean ± SEM.

for humane end points or death. Weekly LNP-h*ARG1* mice demonstrated significant life extension compared with weekly LNP-*luc* control mice ($P < 0.001$), but none exhibited long-term survival and stable weights; all weekly LNP-h*ARG1* mice died or were euthanized for humane end points by day 62, while all weekly LNP-*luc* mice perished by day 27 (Fig. 2 *A* and *B*). In contrast, q3D LNP-h*ARG1* mice exhibited significant life extension ($P < 0.001$) with 100% survival and without physiological signs of hyperammonemia or weight loss to beyond day 77 compared with q3D LNP-*luc* mice, which all perished by day 22 (Fig. 2 *C* and *D*). These data demonstrate that delivery of 2 mg/kg of LNP-h*ARG1* q3D is a therapeutic dose and frequency of administration that can successfully extend and maintain long-term survival and health of arginase-deficient mice. No period of multiday loading of LNP-h*ARG1* by daily injections is necessary (*SI Appendix*, Fig. S1).

Functional Metabolic Recovery of Arg1$^{-/-}$ Mice after Systemic Delivery of LNP-h*ARG1*. To evaluate the metabolic function of conditional Arg1$^{-/-}$ mice in response to LNP-mRNA treatment, plasma was collected over the course of the study and analyzed for various criteria. Due to the transient nature of LNP-mRNA treatment, plasma metabolite levels were expected to fluctuate depending on timing of plasma collection within the therapeutic q3D dosing interval. Therefore, mice ($n = 6$ per group) were bled every 7 d regardless of timing within the dosing interval to collect time points representing the full spectrum within the dosing interval. In weekly LNP-*luc* mice, plasma ammonia levels were measured on day 0 (183.7 ± 26.9 μM) and demonstrated significantly increased concentrations that peaked at death on day 21 (692.9 ± 23.5 μM; $P < 0.001$) (Fig. 3*A*). Similarly, significantly increased plasma ammonia concentrations at death compared with day 0 levels were also found in weekly LNP-h*ARG1* mice (day 0: 120.0 ± 17.8 vs. d 42: 1,409.6 ± 449.5 μM; $P = 0.002$) (Fig. 3*A*) and in q3D LNP-*luc* mice (day 0: 174.1 ± 32.6 vs. d 21: 1505.6 ± 414.5 μM; $P = 0.003$) (Fig. 3*B*). However, q3D LNP-h*ARG1* mice showed good control and no statistically significant increases in plasma ammonia throughout the study compared with day 0 levels, demonstrating amelioration of hyperammonemic episodes induced by hepatic Arg1 disruption (day 0: 112.8 ± 36.7 vs. d 14: 146.2 ± 42.2, day 21: 122.2 ± 35.2, day 28: 130.5 ± 33.4, day 42: 146.5 ± 22.7, day 56: 101.3 ± 31.9, day 70: 123.4 ± 24.5, and day 77: 163.1 ± 33.7 μM; $P > 0.05$) (Fig. 3*B*). Plasma ammonia in mice administered LNP-h*ARG1* q3D was measured at days 0, 14, 21, 28, 42, 56, 70, and 77, demonstrating levels corresponding to 0, 0, 1, 2, 1, 3, 2, and 1 d post-last dose (post-LD), respectively (Fig. 3*B*). Mice ($n = 5$ males per group) administered q3D LNP-h*ARG1* on day 72 (1 d post-LD) were also

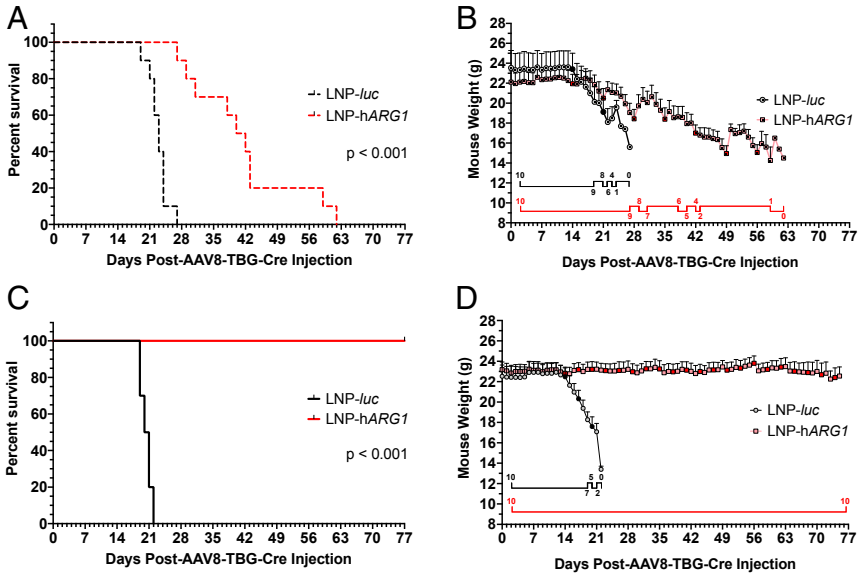

Fig. 2. Survival and weights of conditional ARG1 knockout mice were stable over the long term in mice administered LNP-formulated h*ARG1* mRNA every 3 d. Conditional arginase knockout mice were administered 2×10^{11} genome copies of AAV8-TBG-Cre (day 0) to induce Cre-Lox excision in the endogenous murine Arg1 gene, resulting in loss of function. Mice were administered an IV bolus of 2 mg/kg of LNP-*luc* (control, black line) or 2 mg/kg of LNP-h*ARG1* (experimental, red line) weekly (*A* and *B*) or q3D (*C* and *D*) beginning on day 14. Mice were monitored for survival and clinical evidence of deterioration in both the weekly dosed and q3D-dosed groups up to 11 wk after initiating Cre-Lox recombination ($n = 10$ per group, 5 males and 5 females). (*B* and *D*) Solid black line (LNP-*luc*) and red line (LNP-h*ARG1*) parallel to the *x* axis of weight logs represent surviving animals in each treatment study. (*A* and *C*) $P < 0.001$ obtained by log-rank. Data are presented as mean ± SEM. (*B* and *D*) Day of LNP injection is represented by a darkened red square for LNP-h*ARG1* and solid black circle for LNP-*luc*. g, gram.

able to similarly metabolize an ammonium challenge compared with WT control mice after 60 min, demonstrating an adequate ability to handle exogenous nitrogen loading (Fig. 3*C*).

To further confirm recovery of ureagenesis, q3D LNP-h*ARG1* mice on day 72 (1 d post-LD) and WT control mice ($n = 8$ per group, 4 male and 4 female) were administered intraperitoneal ^{15}N ammonium chloride, which was allowed to metabolize into ^{15}N urea for 60 min before collected blood was measured by gas chromatography-mass spectrometry for ^{15}N urea enrichment (Fig. 3 *D*, *Left*); q3D LNP-h*ARG1* mice metabolized 81.9 ± 11.3% of total WT control ^{15}N urea enrichment levels, demonstrating no statistically significant difference between the 2 groups ($P > 0.05$) (Fig. 3 *D*, *Right*).

Plasma and liver ($n = 6$ per group) were also analyzed for selected amino acids critical to the urea cycle and nitrogen metabolism pathways. Plasma amino acids were measured on days 0, 28, 56, and 77, demonstrating levels corresponding to 0, 2, 3, and 1 d post-LD, respectively. Plasma arginine and glutamine, both typically found elevated in mice with arginase deficiency, were significantly increased at the time of euthanasia in q3D LNP-*luc* mice compared with day 0 (ARG_{D0}: 114.6 ± 1.5 μM vs. ARG_{D21}: 832.5 ± 102.1 μM; $P < 0.001$) (GLN_{D0}: 731.8 ± 47.2 μM vs. GLN_{D21}: 1,277.0 ± 243.0 μM; $P = 0.020$) (Fig. 4 *A* and *B*). However, in q3D LNP-h*ARG1* mice, there was no statistically significant increase in plasma arginine or glutamine observed throughout the course of the study compared with day 0 (ARG_{D0}: 82.3 ± 8.3 μM vs. ARG_{D28}: 127.5 ± 12.09 μM, ARG_{D56}: 165.2 ± 36.47 μM, ARG_{D77}: 151.2 ± 34.4 μM; $P > 0.05$) (GLN_{D0}: 584.5 ± 19.1 μM vs. GLN_{D28}: 643.4 ± 32.5 μM, GLN_{D56}: 628.0 ± 90.86 μM, GLN_{D77}: 784.2 ± 66.7 μM; P = not significant) (Fig. 4 *A* and *B*). Plasma ornithine and lysine were also examined, and while neither the q3D LNP-*luc* group nor the q3D LNP-h*ARG1* group demonstrated statistically significant increases throughout the study, plasma lysine in q3D LNP-*luc* at the time of euthanasia was trending toward statistical significantly increased levels when compared with day 0 (LYS_{D0}: 182.5 ± 21.1 μM vs. LYS_{D21}: 356.9 ± 103.6 μM; $P = 0.096$) (Fig. 4 *C* and *D*).

Hepatic amino acids ($n = 6$ per group unless otherwise noted) were measured for q3D LNP-*luc* mice at the time of euthanasia and for q3D LNP-h*ARG1* mice on day 35 (3 d post-LD) and day 77 (1 d post-LD). Hepatic arginine concentrations in q3D LNP-*luc* mice (34.6 ± 5.7 nmol/mg of protein) were significantly higher compared with q3D LNP-h*ARG1* mice on both day 35 (2.6 ± 1.1 nmol/mg of protein; $P < 0.001$; $n = 4$) and day 77 (3.1 ± 0.2 nmol/mg of protein; $P < 0.001$) and WT control mice (2.5 ± 0.2 nmol/mg of protein; $P < 0.001$) (Fig. 4*E*). Liver glutamine concentrations in q3D LNP-*luc* mice (9.0 ± 1.2 nmol/mg of protein) were significantly lower compared with q3D LNP-h*ARG1* mice on day 77 (26.4 ± 1.8 nmol/mg of protein; $P < 0.001$), but not significantly different from q3D LNP-h*ARG1* mice on day 35 (19.92 ± 4.6 nmol/mg of protein; $P > 0.05$; $n = 4$) or WT control mice (18.0 ± 3.6 nmol/mg of protein; $P > 0.05$) (Fig. 4*F*); ammonia does result in the short-term activation of hepatic glutaminase (35) and may be the cause of this intracellular glutamine reduction in LNP-*luc* mice as plasma ammonia is markedly elevated in this group (Fig. 3*B*). Hepatic ornithine concentrations, when compared with WT controls (2.0 ± 0.2 nmol/mg of protein), were significantly elevated in q3D LNP-*luc* mice (12.1 ± 2.8 nmol/mg of protein; $P = 0.003$) and q3D LNP-h*ARG1* mice on day 35 (11.0 ± 2.3 nmol/mg of protein; $P = 0.017$; $n = 4$), but not significantly elevated in q3D LNP-h*ARG1* mice on day 77 (4.1 ± 0.7 nmol/mg of protein; $P > 0.05$) (Fig. 4*G*). Hepatic lysine concentrations in q3D LNP-*luc* mice (36.2 ± 7.6 nmol/mg of protein) were significantly higher compared with q3D LNP-h*ARG1* mice on both day 35 (7.7 ± 1.8 nmol/mg of protein; $P = 0.002$; $n = 4$) and day 77 (5.9 ± 0.6 nmol/mg of protein; $P < 0.001$) and WT control mice (5.1 ± 0.7 nmol/mg of protein; $P < 0.001$) (Fig. 4*H*).

Guanidino compounds have been found to accumulate in patients with arginase deficiency (6, 8, 36). Therefore, we quantified the accumulation of GAA ($n = 6$ per group unless otherwise stated) in plasma of q3D LNP-*luc* mice at the time of euthanasia and for q3D LNP-h*ARG1* mice on day 35 (3 d post-LD) and day 77 (1 d post-LD). There was no statistically significant increase between q3D LNP-h*ARG1* mice on day 35 (3.9 ± 0.6 nM; $n = 4$) and on day 77 (3.0 ± 0.4 nM) and WT controls (2.3 ± 0.2 nM);

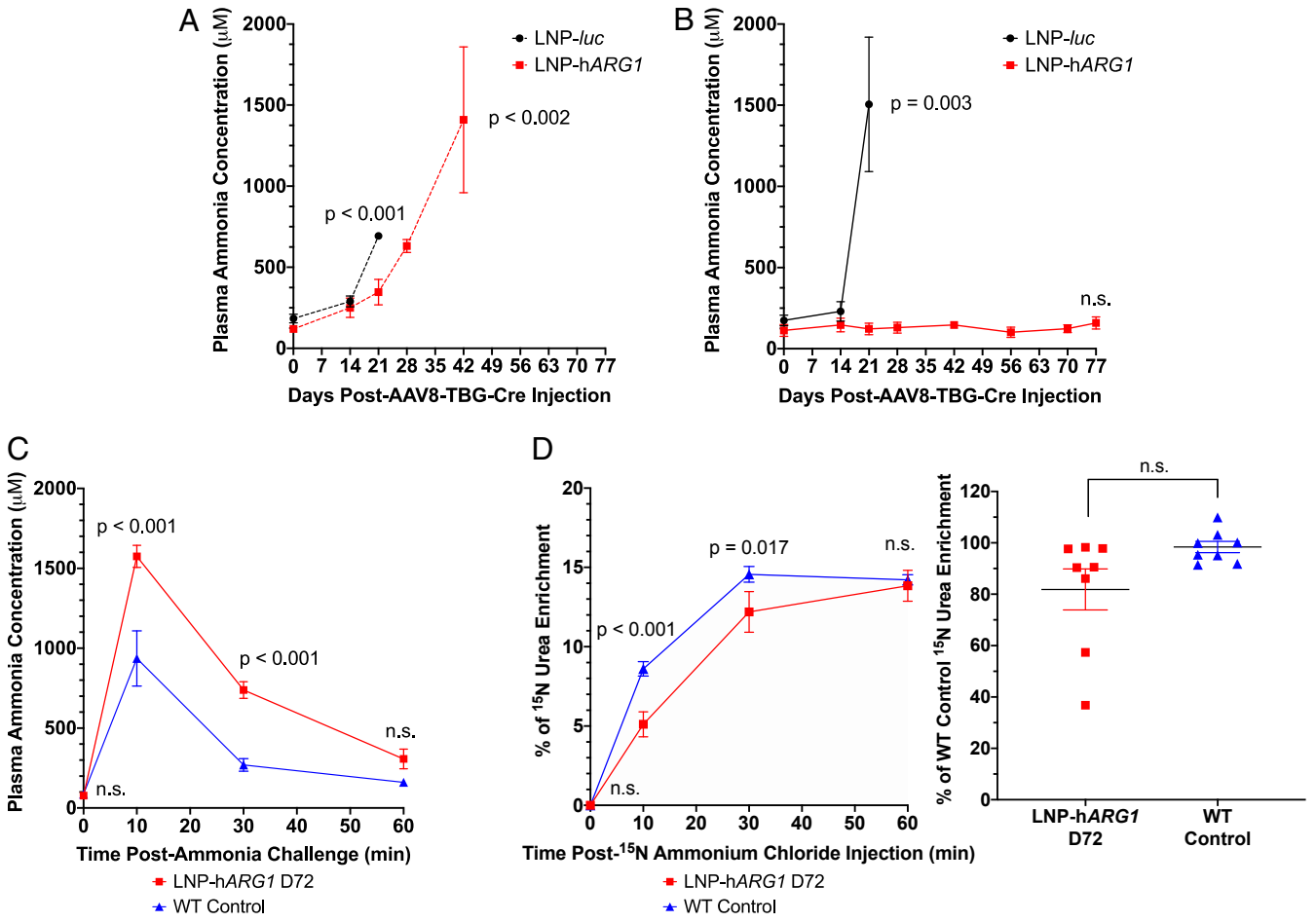

Fig. 3. Administration of LNP-h*ARG1* every 3 d results in controlled plasma ammonia and near-normal ureagenesis. Conditional arginase knockout mice were administered 2×10^{11} genome copies of AAV8-TBC-Cre (day 0) to induce Cre-Lox excision in the endogenous Arg1. Mice were administered an IV bolus of 2 mg/kg LNP-*luc* (control, black line) or 2 mg/kg LNP-h*ARG1* (experimental, red line) weekly (*A*) or q3D (*B*) ($n = 6$ per group) beginning on day 14. (*A*) Plasma ammonia was measured in weekly dosed mice on days 0, 14, 21, 28, and 42 in the morning before subsequent injection of LNP-mRNA in the afternoon ($n = 6$ per group). (*B*) Plasma ammonia was measured in q3D-dosed mice on days 0, 14, 21, 28, 42, 56, 70, and 77, demonstrating levels corresponding to 0, 0, 1, 2, 1, 3, 2, and 1 d post-LD, respectively ($n = 6$ per group). (*C*) q3D LNP-h*ARG1*–treated mice on day 72 (1 d post-LD) (red line; $n = 6$) and WT controls ($Arg1^{flox/flox}$; blue line; $n = 6$) were administered 0.4 M ammonium chloride intraperitoneally (IP), and plasma ammonia was measured 10, 30, and 60 min postchallenge. (*D*) Ureagenesis was assessed at 10, 30, and 60 min after IP administration of 0.4 M ^{15}N ammonium chloride on day 72 (1 d post-LD) in q3D LNP-h*ARG1* and WT control mice by ^{15}N urea enrichment quantitation using gas chromatography-mass spectrometry ($n = 8$ per group). (*Left*) Graph demonstrates the progression of ^{15}N urea enrichment at each time point. (*Right*) Graph demonstrates the total calculated area under the curve to depict the total accumulated quantity of ^{15}N urea enrichment of each group. In this graph, values are normalized to the average total area under the curve value of WT control mice. D, day. In all graphs, *P* values were obtained from 1-way ANOVA with Tukey's multiple comparison test (*A* and *B*), 2-way ANOVA with Sidak's multiple comparison test (*C* and *D*, *Left*), and an unpaired *t* test (*D*, *Right*). Data are presented as mean ± SEM. n.s., not significant.

however, GAA levels of q3D LNP-*luc* mice at the time of euthanasia were trending toward significantly increased levels (3.8 ± 0.6 nM; $P = 0.100$) compared with the WT controls (Fig. 4*I*).

To support the plasma GAA studies, hepatic levels were also quantified for q3D LNP-*luc* mice at the time of euthanasia and for q3D LNP-h*ARG1* mice on day 35 (3 d post-LD) and on day 77 (1 d post-LD) ($n = 4$ per group). Liver GAA levels in q3D LNP-*luc* mice (61.5 ± 12.7 pmol/mg of tissue) were significantly elevated compared with q3D LNP-h*ARG1* mice on day 77 (27.3 ± 6.9 pmol/mg of tissue; $P = 0.047$) and WT controls (18.8 ± 4.3 pmol/mg of tissue; $P = 0.013$); levels were trending toward significance compared with q3D LNP-h*ARG1* mice on day 35 (30.5 ± 5.6 pmol/mg of tissue; $P = 0.077$) (Fig. 4*J*).

To examine for potential liver toxicity induced by long-term administration of LNPs, plasma was examined for levels of alanine aminotransferase (ALT; $n = 6$ per group), a marker of liver injury, in q3D LNP-*luc* mice at the time of euthanasia (49.3 ± 17.5 units [U]/L) and q3D LNP-h*ARG1* mice on D77 (1 d post-LD) (33.6 ± 3.8 U/L); differences in levels in both groups were not statistically significant compared with WT control levels (27.3 ± 3.7 U/L) ($P > 0.05$ for both comparisons) (Fig. 4*K*). Altogether, these data demonstrate the ability for this treatment modality to completely and safely recover the metabolic profile of adult arginase-deficient mice.

LNP-h*ARG1* Levels and Localization Characteristics within $Arg1^{-/-}$ Livers. After the completion of our in vivo and plasma biochemical studies, LNP-mRNA–treated mice were euthanized and their livers were collected, sectioned, and analyzed to characterize LNP-h*ARG1* levels and distribution. The h*ARG1* mRNA in LNP-mRNA–treated livers was determined relative to the murine *Gapdh* housekeeping transcript levels ($n = 6$ per group). The q3D LNP-h*ARG1* mice were euthanized on day 77 (1 d post-LD). Mice were found to have a markedly and significantly increased level of h*ARG1* mRNA compared with LNP-*luc* and WT control mice ($P = 0.022$ for both) (Fig. 5*A*). In contrast, weekly LNP-h*ARG1*

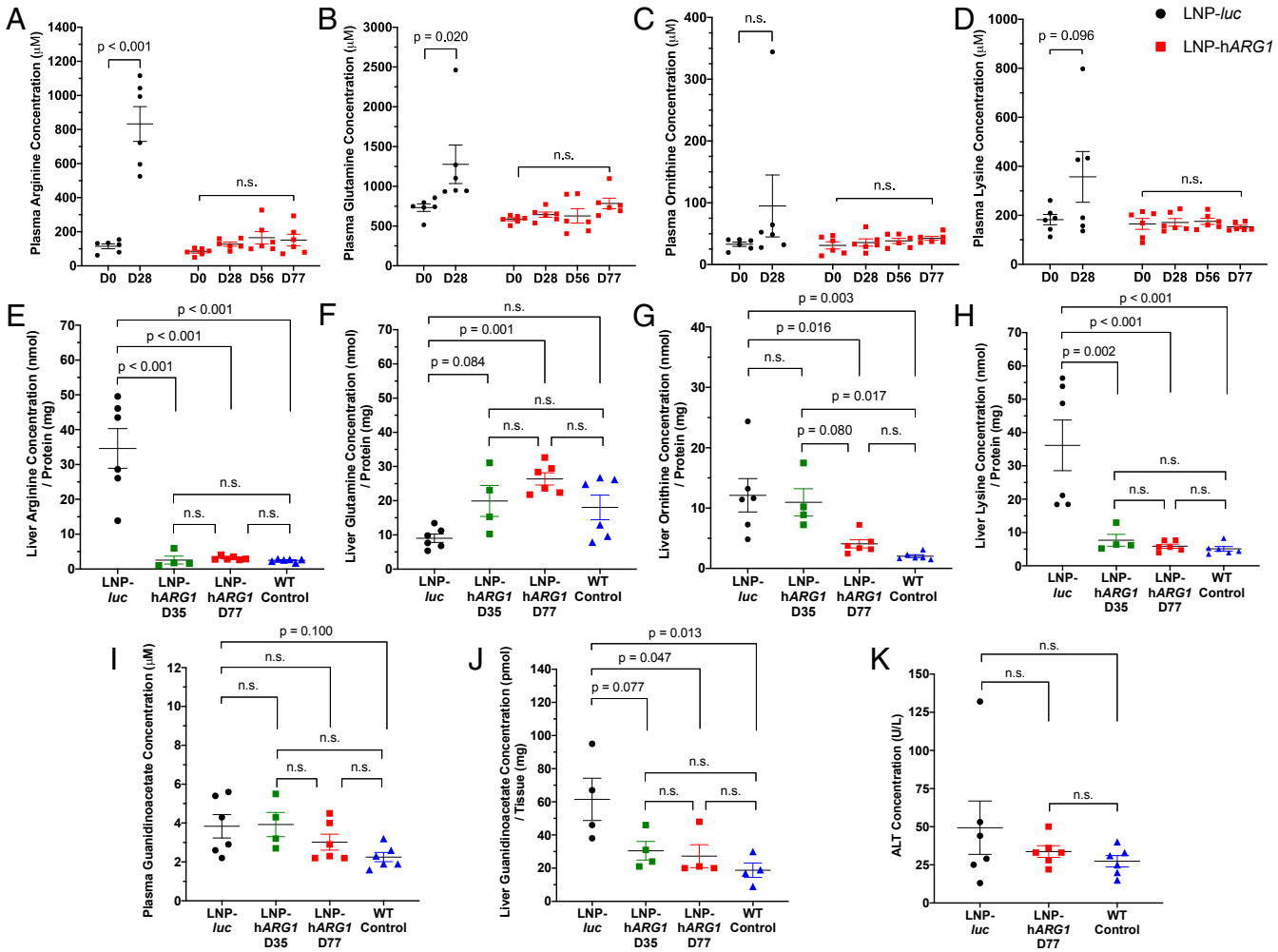

Fig. 4. LNP-h*ARG1* administration every 3 d prevents elevated plasma and hepatic arginine, controls plasma glutamine, and prevents GAA accumulation in the plasma. Plasma arginine (*A*), glutamine (*B*), ornithine (*C*), and lysine (*D*) were assessed in q3D control LNP-*luc* mice ($n = 6$; black) at days 0 and 28 and in q3D LNP-h*ARG1* mice ($n = 6$; red) at days 0, 28, 56, and 77, demonstrating levels corresponding to 0, 2, 3, and 1 d post-LD, respectively. Hepatic arginine (*E*), glutamine (*F*), ornithine (*G*), and lysine (*H*) were similarly assessed in control q3D LNP-*luc* mice at the time of euthanasia ($n = 6$; black) and in q3D LNP-h*ARG1* mice on day 35 (3 d post-LD; $n = 4$; green) and on day 77 (1 d post-LD; $n = 6$; red) and compared with WT control liver ($n = 6$; blue). (*I*) Plasma guanidino compounds, represented by GAA, were assessed in q3D LNP-h*ARG1* mice on day 35 (3 d post-LD; $n = 4$; green) and on day 77 (1 d post-LD; $n = 6$; red) and compared with q3D LNP-*luc* mice ($n = 6$; black) and WT controls ($n = 6$; blue). (*J*) Liver GAA was assessed using a method similar to that in *I* ($n = 4$ per group). (*K*) Plasma ALT was assessed in q3D LNP-h*ARG1* on day 77 (1 d post-LD; $n = 6$; red) and compared with q3D LNP-*luc* at the time of euthanasia ($n = 6$; black) and in WT controls ($n = 6$; blue). In all graphs, *P* values were obtained from 1-way ANOVA with Tukey's multiple comparison test. Data are presented as mean ± SEM. D, day; n.s., not significant.

mice showed levels of h*ARG1* mRNA in large variation and demonstrated no statistically significant differences compared with weekly LNP-*luc* and WT control mice (*SI Appendix*, Fig. S2*A*).

Liver lysates from LNP-mRNA–treated mice ($n = 6$ per group) were analyzed for functional ARG1 protein. The q3D LNP-h*ARG1* mice on day 77 (1 d post-LD) recovered 53.6 ± 6.3% of functional ARG1 activity relative to WT control mice ($P < 0.001$) (Fig. 5*B*). In contrast, while weekly LNP-h*ARG1* mice at time of euthanasia recovered 10.9 ± 1.5% of functional ARG1 activity relative to WT control mice ($P < 0.001$), these activity levels were found to be not significantly different from those of weekly LNP-*luc* mice at the time of euthanasia with 6.4 ± 0.6% of functional ARG1 activity ($P > 0.05$), whose expression was too low to maintain survival (*SI Appendix*, Fig. S2*B*). To further confirm these findings, Western blot analysis was performed with q3D LNP-h*ARG1* liver collected on day 77 (1 d post-LD), which revealed the strong presence of a single 35-kilodalton (kDa) isoform of ARG1 derived from LNP-h*ARG1* compared with WT mouse liver that demonstrates both 35- and 37-kDa endogenous Arg1 isoforms (Fig. 5*C*). Weekly LNP-h*ARG1* livers collected at the time of euthanasia demonstrated a minimal presence of ARG1 protein (*SI Appendix*, Fig. S2*C*).

To confirm that any survival extension was due to LNP-h*ARG1* treatment and not to maintenance of endogenous murine Arg1 expression, qRT-PCR primers were designed to span the endogenous murine *Arg1* exon 7 and 8 mRNA junction excised after AAV8-TBG-Cre activation. In weekly LNP-mRNA–treated and q3D LNP-*luc*–treated livers collected at the time of euthanasia and in q3D LNP-h*ARG1*–treated mice on day 77 (1 d post-LD), there was an absence of endogenous murine *Arg1* mRNA compared with WT control levels ($P > 0.05$ for both) (*SI Appendix*, Fig. S2 *D* and *E*).

Livers collected from weekly LNP-h*ARG1* and q3D LNP-*luc* mice collected at the time of euthanasia and from q3D LNP-h*ARG1* mice on day 77 (1 d post-LD) were sectioned and underwent various imaging analyses. The presence of h*ARG1* mRNA in LNP-mRNA–treated livers was visualized using in situ hybridization (ISH) probes designed specifically for h*ARG1* mRNA that

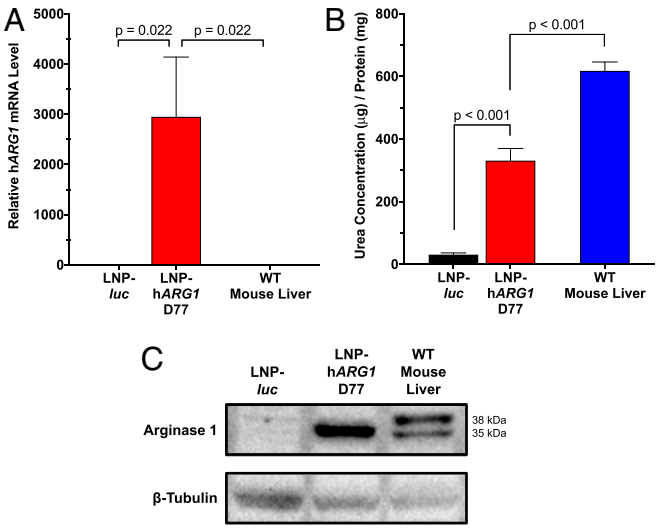

Fig. 5. LNP-h*ARG1* administration results in restoration of hepatic arginase mRNA and protein. The h*ARG1* mRNA hepatic levels relative to the murine *Gapdh* housekeeping gene were assessed by qRT-PCR (A), and functional hepatic ARG1 activity was assessed by a biochemical functional arginase assay (*B*) q3D in LNP-h*ARG1* mice on day 77 (1 d post-LD) and compared with q3D LNP-*luc* at the time of euthanasia and in WT controls ($n = 6$ per group). (*C*) Western blot analysis of hepatic ARG1 transgene expression in q3D LNP-h*ARG1* mice on day 77 (1 d post-LD) was compared with q3D LNP-*luc* at the time of euthanasia and in WT control liver. *P* values were obtained from 1-way ANOVA with Tukey's multiple comparison test. Data are presented as mean ± SEM. D, day.

was LNP-encapsulated. ISH of q3D LNP-h*ARG1* livers on day 77 collected 24 h after the final LNP-h*ARG1* dose revealed a positive but low presence of h*ARG1* mRNA in both hepatocytes and Kupffer cells (Fig. 6); h*ARG1* mRNA levels were in accordance with previous PK data that demonstrated a significant reduction in h*ARG1* mRNA after 24 h post–LNP-h*ARG1* injection (Fig. 1*C*). Weekly LNP-h*ARG1* mice similarly euthanized 24 h after the final LNP-h*ARG1* dose also demonstrated the positive, but lower, presence of h*ARG1* mRNA compared with q3D LNP-h*ARG1* livers by ISH (*SI Appendix*, Fig. S3). Immunofluorescent staining for ARG1 and glutamine synthetase (GS), to differentiate periportal ($GS^{Negative}$) and perivenous ($GS^{Positive}$) vasculature, was performed on weekly and q3D LNP-mRNA–treated liver sections to visualize localization of ARG1 expression. For weekly LNP-h*ARG1* livers collected at the time of euthanasia, no expression of ARG1 could be visualized, further confirming results from the molecular analysis (*SI Appendix*, Fig. S3). However, q3D LNP-h*ARG1* livers on day 77 (1 d post-LD) revealed strong ARG1 expression primarily localized in the periportal and interportal spaces consistent with LNP-h*ARG1* hepatic entrance via periportal vasculature and diffusion out to peripheral hepatocytes (Fig. 6). All liver sections were also stained with hematoxylin/eosin (H&E), revealing no overt pathological hepatic abnormalities or lymphocytic infiltrates, and with Masson's trichrome, where the absence of dark blue staining indicated lack of hepatic fibrosis or collagen deposition (Fig. 6). Furthermore, liver sections were imaged by electron microscopy to reveal intricate subcellular structures. All groups showed regular organization of the hepatic tissue without evidence of accumulation of electron-dense inclusions or bundles of collagen fibers. Hepatocytes demonstrated normal nuclear membranes, rough endoplasmic reticulum, and mitochondrial morphology. Compared with the WT and LNP-h*ARG1*–treated mice, LNP-*luc* hepatocytes did reveal mitochondria that were slightly enlarged (Fig. 6 and *SI Appendix*, Fig. S3) and the occasional presence of a lipid droplet (Fig. 6, arrows).

Discussion

UCDs are a family of inherited metabolic conditions of the liver in any of 6 enzymes or 2 transporters that impair ureagenesis and normal nitrogen detoxification produced as a consequence of protein metabolism (37). They are caused by monogenic loss of enzyme or transporter function, and are combined with straightforward medical treatments (i.e., protein-restricted diet, ammonia scavengers) that do not address the underlying cause. UCDs can result in the rapid development of hyperammonemia characterized by symptoms and signs, including headaches, hypo/hyperventilation, seizures, coma, and potentially death (38). Survivors typically have intellectual disabilities and remain vulnerable to repeat episodes of hyperammonemia with their cumulative and permanent neurological injury.

Arginase deficiency (OMIM:207800), caused by biallelic mutations in ARG1, tends to be recognized in late infancy to early childhood, unlike the other UCDs, where hyperammonemia and related signs often occur within a few days of birth (4, 38). Often identified by a presentation of spastic paraparesis or quadriparesis, the condition has progressive neurological decline, including developmental delays, psychomotor and growth retardation, and seizures as characteristic findings (4). While the potential for

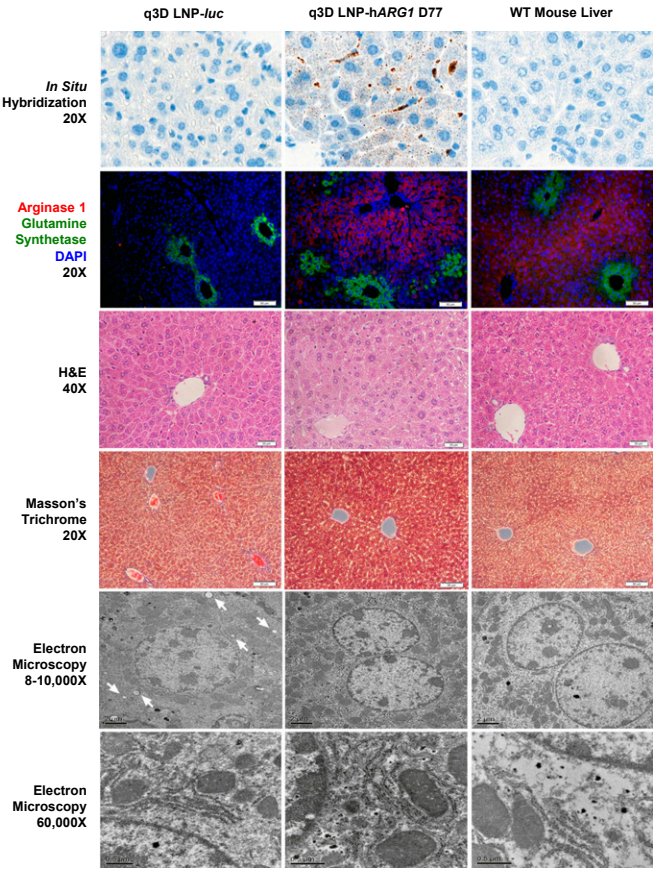

Fig. 6. LNP-h*ARG1*–mediated protein is detected in the liver when administered by LNP without evidence of inflammatory infiltrates, fibrosis, or subcellular injury. Liver sections of representative images of q3D LNP-*luc* mice at the time of euthanasia, q3D LNP-h*ARG1* mice on day 77 (1 d post LD), and WT control mice were examined for h*ARG1* mRNA presence by ISH (RNAScope) (first row, 20× magnification), for ARG1 transgene expression with greater perivenous vascular localization by immunostaining for ARG1 (red) and GS (green) (second row, 20× magnification), for hepatic histology by H&E staining (third row, 40× magnification); for collagen deposition/fibrosis by Masson's trichrome staining (fourth row, 20× magnification), and by electron microscopy (fifth row, 8,000× to 10,000× magnification; sixth row, 60,000× magnification). Arrows denote lipid droplets.

diagnosis by newborn screening would enable earlier therapeutic intervention (39), the current treatment is less than fully effective at best, resulting in progressive neurological injury. As such, arginase deficiency is another example of the growing number of metabolic diseases that can be detected by newborn screening but lack fully effective therapies.

In these present studies, we asked the question whether encapsulation of h*ARG1* mRNA within liver-targeting LNPs and their systemic delivery to arginase-deficient mice can achieve therapeutic recovery of urea cycle function at a reasonable concentration, dosage, and frequency and result in normal biochemical parameters. We demonstrate that administration of 2 mg/kg of LNP-h*ARG1* every 3 d results in both biochemical and functional efficacy of h*ARG1* mRNA. Unlike ARG1-deficient mice treated with a control mRNA (2 mg/kg of LNP-*luc* q3D), where all mice perished by day 22, we achieved 100% survival beyond 11 wk, stable weight, and recovery of urea cycle function with LNP-h*ARG1*, as demonstrated, in part, by maintenance of normal plasma ammonia and urea cycle-related amino acid levels, including glutamine. Notably, maintenance of normal plasma ammonia and amino acid levels was sustained throughout the q3D dosing interval with analysis occurring 1, 2, and 3 d post-LD. Importantly, unlike some other metabolic disorders where restored hepatic expression results in incomplete correction due to other metabolite-producing uncorrected tissues [e.g., methylmalonic acidemia (40)], plasma arginine was completely normalized as the urea cycle is exclusive to the liver. In addition, the generation of disease-related metabolites (i.e., GAA) is prevented, and repeat administration of h*ARG1* mRNA led to stable weights, an indication of the overall health of the mice. The distribution of the exogenous arginase protein was panhepatic, as occurs naturally, and is in contrast to the other urea cycle enzymes that concentrate in the periportal areas.

PK studies revealed the LNP as an effective delivery vehicle of h*ARG1* mRNA in vivo, leading to peak levels of h*ARG1* mRNA in the liver shortly after administration. Significant degradation of LNP-mRNA within 24 h is consistent with other studies (40). Functionally, whereas control mice demonstrated no hepatic arginase activity and perished, translated ARG1 protein from LNP-h*ARG1* persisted even after significant h*ARG1* mRNA degradation, leading to 54% of normal hepatic arginase activity 24 h after administration. This led to mice (1 d post-LD) being able to completely metabolize an exogenous challenge of ammonia into urea. In addition, ureagenesis was reestablished with similar ^{15}N incorporation in mice (1 d post-LD) compared with WT mice. While analyses aimed to quantify h*ARG1* mRNA and translated protein levels in the liver, as well as in vivo efficacy of LNP-h*ARG1* through exogenous ammonia challenges and recovery of ureagenesis, were performed on mice 1 d post-LD, a time point expected to have high ARG1 expression, we nonetheless have demonstrated the sustained efficacy of LNP-h*ARG1* throughout the q3D dosing interval, as evidenced by maintenance of normal weight, plasma amino acids, and prevention of GAA accumulation in mice 3 d post-LD.

LNP-h*ARG1* also led to normalization of intracellular arginine levels in hepatocytes; this is not achievable with enzyme replacement therapy (presently in clinical trial NCT03378531) due to the inability of the PEGylated enzyme to enter hepatocytes (11). Although further studies need to be performed, we hypothesize that normalization of intrahepatic arginine levels (not only plasma arginine levels) is needed to avoid the accumulation of disease-related metabolites such as GAA.

With concern for long-term toxicity issues related to repeat dosing of LNPs, we demonstrated that at the end of the 11-wk study, there was no histological or enzymatic evidence of liver injury. Further examination with electron microscopy demonstrated hepatocytes with normal nuclear membranes, rough endoplasmic reticulum, and mitochondrial morphology. Taken together, within the duration and scope of our study, repeat LNP-h*ARG1* dosing allowed for long-term survival and maintenance of normal plasma ammonia without evidence of hepatocellular injury.

We did find better survival and normalization of plasma ammonia during the q3D dosing period than with weekly administration. Whereas human arginase-deficient patients uncommonly have hyperammonemia, the murine model presents with both hyperammonemia and hyperargininemia, with the former leading to death. In this model, the q3D dosing is needed for extended therapeutic efficacy and survival. Along with q3D dosing, we examined 2 mg/kg of LNP-h*ARG1* administered weekly and demonstrated significant life extension; however, the weekly dosed mice exhibited unstable weights and significant increases of plasma ammonia by the end of each week, and they eventually succumbed to hyperammonemia. Notably, some weekly dosed mice had the positive presence of h*ARG1* mRNA by the time of death or euthanasia; however, Western blot and a functional assay demonstrated minimal hARG1 protein expression, potentially due to inadequate time for proper protein translation and the progression of disease in the mice. Thus, while further frequency optimization will be necessary for clinical application, human patients may not require the frequency of administration utilized in these murine studies.

Although progress has been made by way of advancements with both integrating and nonintegrating viral vector- and non–viral-based technologies to restore enzyme function, these gene therapy methods, for arginase deficiency, generally remain in the preclinical stage (16, 17, 41) and exhibit potential disadvantages. These include risk for insertional mutagenesis (24) and limited efficacy due to hepatocellular division (25) with viral-based strategies, lack of availability of cellular-based strategies (42) and organ-based strategies (43), and inability for hepatocyte penetrance with PEGylated enzyme replacement (11). Although highly promising and potentially curative, these strategies must be studied further to ensure effectiveness and safety before consideration of clinical applicability. Delivering mRNA to the liver is an alternative strategy to provide missing or defective enzyme function. The ability to repeatedly dose LNPs that carry h*ARG1* mRNA, supported by the PK studies that demonstrate rapid onset of expression and the tolerability of multiple dosing, suggests the value and preclinical proof-of-concept efficacy of LNP-based ARG1 mRNA therapy as an effective therapy for arginase deficiency.

Materials and Methods

Mouse Procedures. Conditional arginase-deficient mice on a C57BL/6 background (stock no. 008817; The Jackson Laboratory) were housed under specific pathogen-free conditions with food and water provided ad libitum. All mice were kept according to NIH guidelines, and all experimental procedures were conducted in accordance with guidelines for the care and use of research animals by the Chancellor's Animal Research Committee at the University of California, Los Angeles. At day 0, 8- to 12-wk-old animals were IV administered 2.0×10^{11} genome copies of AAV8-TBG-Cre (University of Pennsylvania Vector Core, Philadelphia, PA) prepared in sterile pharmaceutical grade saline. Male and female mice were distributed evenly throughout the study unless otherwise stated. Scheduled blood collections were taken from the retroorbital plexus under isoflurane anesthesia. Plasma was frozen immediately and stored at −80 °C. Mice were euthanized if they showed symptoms of lethargy, lying on their side, or inability to right themselves as signs of hyperammonemia. Beginning day 14 after AAV8-TBG-Cre injection, mice were administered IV LNP-encapsulated mRNA prepared at 2 mg/kg in sterile phosphate-buffered saline (PBS). One group of mice was injected with LNP-mRNA weekly, while 2 groups were injected every 3 d, one of which also received daily LNP-mRNA loading from days 14 to 21.

mRNA Synthesis and Formulation. The h*ARG1* mRNA codon optimization was performed using typical methods in the field (44). The mRNAs encoding luciferase and h*ARG1* were synthesized in vitro by T7 RNA polymerase-mediated transcription using a linearized DNA template that incorporated both the 5′ and 3′ untranslated regions with a poly-A tail and then purified and formulated for IV delivery as previously described (45) (the open reading frame for h*ARG1* is provided in *SI Appendix*).

BLI. Mice were shaved prior to imaging to minimize absorption of light by black fur and then imaged; total flux values in photons per second were calculated as previously described (25).

ALT Analysis. ALT level determination was performed from plasma samples using a Vet Excel Clinical Chemistry Analyzer (Alfa Wassermann Diagnostic Technologies) per the manufacturer's instructions.

Ammonia Analysis. Ammonia determination was performed in duplicate from plasma samples per the manufacturer's instructions (Abcam). Prolonged storage of plasma was avoided, and testing was generally performed with all samples simultaneously to avoid any batch effect.

Plasma and Liver Amino Acids. The concentration of amino acids in plasma and liver was determined by high performance liquid chromatography as previously described (46).

Guanidino Compounds. The concentration of GAA in the plasma and liver was determined by using a normal phase hydrophilic interaction column after analyte derivatization as previously described (47).

Ammonia Challenge and Ureagenesis. Mice were fasted for 3 to 4 h prior to the beginning of ammonia challenging, as previously described (23), using 4 mmol/kg of ^{15}N ammonium chloride ($^{15}NH_4Cl$; Cambridge Isotope Laboratories). Blood collections were performed immediately before and at 10, 30, and 60 min after injection, also allowing for ureagenesis determination as previously described (48).

Functional Arginase Analysis. Hepatic arginase activity was measured in duplicate from liver tissue lysates as previously described (16).

Histology and Immunohistochemistry. Liver tissues were fixed in 10% (vol/vol) buffered formalin for 48 h and then stored in 70% ethanol. Fixed tissue was embedded in paraffin blocks using standard procedures from which 4-μm-thick sections were collected on microscope slides. Section deparaffinization, rehydration, antigen retrieval, and permeabilization were performed as previously described (46). Sections were blocked with 10% (vol/vol) normal goat serum in PBS for 30 min. Sections were coincubated with primary antibodies for arginase (sc-20150; Santa Cruz Biotechnology) and GS (ab64613; Abcam) overnight at 4 °C. Sections were then coincubated with the fluorescent antibodies donkey anti-goat Alexa Fluor 594 (A11058; Invitrogen) and goat anti-mouse Alexa Fluor 488 (A11001; Invitrogen) for 1 h at room temperature. Section cell nuclei were counterstained with DAPI, mounted with VECTASHIELD Antifade Mounting Medium with DAPI (Vector Laboratories), and then visualized.

H&E and Masson's trichrome staining was performed by standard methods.

mRNA ISH. mRNA ISH was performed using RNAScope technology on an automated Leica BOND RX autostainer platform using the RNAScope 2.5 LS Reagent Kit-BROWN from Advanced Cell Diagnostics (ACD). An exclusive target probe with proprietary sequences was designed by ACD to target ARG1 mRNA. Control probes to the housekeeping gene *Mus musculus* peptidylprolyl isomerase B mRNA (catalog no. 313918; ACD), as a positive control, or the bacterial gene dihydrodipicolinate reductase (catalog no. 312038; ACD), as a negative control, was also used as a quality control check for tissues. Slides were processed using a Leica staining protocol per the user manual (document no. 322100-USM; ACD). All images were captured at 20× magnification with the Panoramic 250 Flash II (3DHISTECH) digital slide scanner.

Electron Microscopy. Four groups of liver tissues were collected and fixed in 4% (vol/vol) paraformaldehyde (Electron Microscopy Sciences) plus 2.5% (vol/vol) glutaraldehyde (Thermo Fisher Scientific) in PBS solution at 4 °C for several weeks. Each liver sample was prepared for imaging by standard methods (details of the methods used are provided in *SI Appendix*).

RNA Isolation. Total RNA was isolated from ∼20 mg of homogenized liver tissue with a Roche High Pure RNA Isolation Kit (Roche Applied Sciences) per the manufacturer's instructions.

Residual Endogenous Murine Arg1 mRNA qRT-PCR. One microgram of total RNA was reverse-transcribed to cDNA with a Transcriptor First Strand cDNA Synthesis Kit (Roche Applied Sciences) per the manufacturer's instructions. Primers for endogenous murine *Arg1* mRNA were designed to bind to the exon 7/8 junction: forward primer 5′-ACATCACAGAAGAAATTTACAAGACAG/reverse primer 5′-TGCCGTGTTCACAGTACTCTTC, with an amplicon length of 113 nucleotides. After cDNA synthesis, qRT-PCR was performed using SsoAdvanced Universal SYBR Green Supermix (Bio-Rad) on a MyiQ2 Two-Color Real-Time PCR Detection System (Bio-Rad). Transcript levels were analyzed in triplicate using the C_T (threshold cycle) values. Target transcript levels were normalized to endogenous murine *β-Actin* mRNA, and fold enrichment was measured using the $2^{-\Delta\Delta Ct}$ method.

h*ARG1* mRNA qRT-PCR. Total RNA was diluted to 10 ng/μL in water. LNP-encapsulated mRNA quantification was performed in triplicate with a Taqman RNA-to-CT 1 Step Kit (Thermo Fisher Scientific) per the manufacturer's instructions. For relative quantification of h*ARG1* mRNA, sample mRNA quantification was calculated relative to the Taqman-validated primer/probe pair for the murine *Gapdh* housekeeping gene (catalog no. 4331182, assay ID no. Hs02786624_g1; Thermo Fisher Scientific) using the $2^{-\Delta\Delta Ct}$ method, with ARG1 forward primer: CAAGGACATCGTCTACATCGG/reverse primer: ACCTCGGTCATGGAGAAGTA.

Western Blot. Liver tissue was homogenized, and 50 μg of protein was transferred and coincubated with the target primary arginase antibody (sc-20150; Santa Cruz Biotechnology) and the loading control primary antibody β-tubulin (sc-9104; Santa Cruz Biotechnology), followed by incubation with secondary horseradish peroxidase-conjugated goat anti-rabbit antibody (sc-2004; Santa Cruz Biotechnology). (details are provided in *SI Appendix*).

Statistical Analysis. All collected data were analyzed with the GraphPad Prism8 statistical package. Results were expressed as mean ± SEM, and *P* values were determined using 1-way ANOVA with Tukey's multiple comparison test, 2-way ANOVA with Sidak's multiple comparison test, or an unpaired *t* test when applicable. Error bars represent SEM. $P < 0.05$ was considered significant.

ACKNOWLEDGMENTS. We are grateful for the performance of the amino acid profiles by Drs. Itzhak and Ilana Nissim (Metabolomics Core facility, The Children's Hospital of Philadelphia; https://metabolomic.research.chop.edu/) and for the determination of plasma guanidino acetoacetate by Dr. Qin Sun (Baylor Genetics). We also thank Sarah Pyle for the illustrations included in Fig. 1. The studies were supported by NIH Grant 5 R01 NS100979-03 (to G.S.L.). We acknowledge the use of instruments at the Electron Imaging Center for NanoMachines supported by NIH Grant 1S10RR23057 (to Z. Hong Zhou) and the California NanoSystems Institute at UCLA.

1. M. L. Summar *et al.*; European Registry and Network for Intoxication Type Metabolic Diseases (E-IMD); Members of the Urea Cycle Disorders Consortium (UCDC), The incidence of urea cycle disorders. *Mol. Genet. Metab.* **110**, 179–180 (2013).
2. S. D. Cederbaum *et al.*, Arginases I and II: Do their functions overlap? *Mol. Genet. Metab.* **81** (suppl. 1), S38–S44 (2004).
3. T. Uchino *et al.*, Molecular basis of phenotypic variation in patients with argininemia. *Hum. Genet.* **96**, 255–260 (1995).
4. D. R. Carvalho *et al.*, Clinical features and neurologic progression of hyperargininemia. *Pediatr. Neurol.* **46**, 369–374 (2012).
5. J. L. Deignan *et al.*, Guanidino compound levels in blood, cerebrospinal fluid, and post-mortem brain material of patients with argininemia. *Mol. Genet. Metab.* **100** (suppl. 1), S31–S36 (2010).
6. B. Marescau *et al.*, Guanidino compounds in plasma, urine and cerebrospinal fluid of hyperargininemic patients during therapy. *Clin. Chim. Acta* **146**, 21–27 (1985).
7. N. Mizutani *et al.*, Guanidino compounds in hyperargininemia. *Tohoku J. Exp. Med.* **153**, 197–205 (1987).
8. P. Wiechert *et al.*, Excretion of guanidino-derivates in urine of hyperargininemic patients. *J. Genet. Hum.* **24**, 61–72 (1976).
9. P. Wiechert, B. Marescau, P. P. De Deyn, A. Lowenthal, Hyperargininemia, epilepsy and the metabolism of guanidino compounds. *Padiatr. Grenzgeb.* **28**, 101–106 (1989).
10. J. L. Deignan *et al.*, Increased plasma and tissue guanidino compounds in a mouse model of hyperargininemia. *Mol. Genet. Metab.* **93**, 172–178 (2008).
11. L. C. Burrage *et al.*; Members of Urea Cycle Disorders Consortium, Human recombinant arginase enzyme reduces plasma arginine in mouse models of arginase deficiency. *Hum. Mol. Genet.* **24**, 6417–6427 (2015).
12. E. Santos Silva *et al.*, Liver transplantation in a case of argininaemia. *J. Inherit. Metab. Dis.* **24**, 885–887 (2001).
13. E. S. Silva *et al.*, Liver transplantation prevents progressive neurological impairment in argininemia. *JIMD Rep.* **11**, 25–30 (2013).
14. R. K. Iyer *et al.*, Mouse model for human arginase deficiency. *Mol. Cell. Biol.* **22**, 4491–4498 (2002).
15. C. L. Gau *et al.*, Short-term correction of arginase deficiency in a neonatal murine model with a helper-dependent adenoviral vector. *Mol. Ther.* **17**, 1155–1163 (2009).
16. E. K. Lee *et al.*, Long-term survival of the juvenile lethal arginase-deficient mouse with AAV gene therapy. *Mol. Ther.* **20**, 1844–1851 (2012).
17. C. Hu *et al.*, Myocyte-mediated arginase expression controls hyperargininemia but not hyperammonemia in arginase-deficient mice. *Mol. Ther.* **22**, 1792–1802 (2014).

18. G. S. Lipshutz, R. Sarkar, L. Flebbe-Rehwaldt, H. Kazazian, K. M. Gaensler, Short-term correction of factor VIII deficiency in a murine model of hemophilia A after delivery of adenovirus murine factor VIII in utero. *Proc. Natl. Acad. Sci. U.S.A.* **96**, 13324–13329 (1999).
19. S. DeWeerdt, Prenatal gene therapy offers the earliest possible cure. *Nature* **564**, S6–S8 (2018).
20. C. Hu, G. S. Lipshutz, AAV-based neonatal gene therapy for hemophilia A: Long-term correction and avoidance of immune responses in mice. *Gene Ther.* **19**, 1166–1176 (2012).
21. S. N. Waddington *et al*., Fetal and neonatal gene therapy: Benefits and pitfalls. *Gene Ther.* **11** (suppl. 1), S92–S97 (2004).
22. G. Cantero *et al*., Rescue of the functional alterations of motor cortical circuits in arginase deficiency by neonatal gene therapy. *J. Neurosci.* **36**, 6680–6690 (2016).
23. E. K. Lee *et al*., AAV-based gene therapy prevents neuropathology and results in normal cognitive development in the hyperargininemic mouse. *Gene Ther.* **20**, 785–796 (2013).
24. R. J. Chandler *et al*., Vector design influences hepatic genotoxicity after adeno-associated virus gene therapy. *J. Clin. Invest.* **125**, 870–880 (2015).
25. C. Hu, R. W. Busuttil, G. S. Lipshutz, RH10 provides superior transgene expression in mice when compared with natural AAV serotypes for neonatal gene therapy. *J. Gene Med.* **12**, 766–778 (2010).
26. Z. Wang *et al*., Adeno-associated virus serotype 8 efficiently delivers genes to muscle and heart. *Nat. Biotechnol.* **23**, 321–328 (2005).
27. S. C. Cunningham, A. P. Dane, A. Spinoulas, G. J. Logan, I. E. Alexander, Gene delivery to the juvenile mouse liver using AAV2/8 vectors. *Mol. Ther.* **16**, 1081–1088 (2008).
28. N. Fausto, J. S. Campbell, The role of hepatocytes and oval cells in liver regeneration and repopulation. *Mech. Dev.* **120**, 117–130 (2003).
29. Y. Magami *et al*., Cell proliferation and renewal of normal hepatocytes and bile duct cells in adult mouse liver. *Liver* **22**, 419–425 (2002).
30. S. Ramaswamy *et al*., Systemic delivery of factor IX messenger RNA for protein replacement therapy. *Proc. Natl. Acad. Sci. U.S.A.* **114**, E1941–E1950 (2017).
31. D. An *et al*., Systemic messenger RNA therapy as a treatment for methylmalonic acidemia. *Cell Rep.* **24**, 2520 (2018).
32. M. S. Kormann *et al*., Expression of therapeutic proteins after delivery of chemically modified mRNA in mice. *Nat. Biotechnol.* **29**, 154–157 (2011).
33. T. S. Zatsepin, Y. V. Kotelevtsev, V. Koteliansky, Lipid nanoparticles for targeted siRNA delivery–Going from bench to bedside. *Int. J. Nanomedicine* **11**, 3077–3086 (2016).
34. J. Kasten *et al*., Lethal phenotype in conditional late-onset arginase 1 deficiency in the mouse. *Mol. Genet. Metab.* **110**, 222–230 (2013).
35. M. I. Chung-Bok, M. Watford, Characterization of the hepatic glutaminase promoter. *Contrib. Nephrol.* **121**, 43–47 (1997).
36. W. Amayreh, U. Meyer, A. M. Das, Treatment of arginase deficiency revisited: Guanidinoacetate as a therapeutic target and biomarker for therapeutic monitoring. *Dev. Med. Child Neurol.* **56**, 1021–1024 (2014).
37. A. Jichlinski, L. Clarke, M. T. Whitehead, A. Gropman, "Cerebral palsy" in a patient with arginase deficiency. *Semin. Pediatr. Neurol.* **26**, 110–114 (2018).
38. N. Ah Mew *et al*., "Urea cycle disorders overview" in *GeneReviews*, M. P. Adam *et al*., Eds. (University of Washington, Seattle, 2003).
39. B. L. Therrell, R. Currier, D. Lapidus, M. Grimm, S. D. Cederbaum, Newborn screening for hyperargininemia due to arginase 1 deficiency. *Mol. Genet. Metab.* **121**, 308–313 (2017).
40. R. J. Chandler *et al*., Metabolic phenotype of methylmalonic acidemia in mice and humans: The role of skeletal muscle. *BMC Med. Genet.* **8**, 64 (2007).
41. C. Hu *et al*., Minimal ureagenesis is necessary for survival in the murine model of hyperargininemia treated by AAV-based gene therapy. *Gene Ther.* **22**, 111–115 (2015). Correction in: *Gene Ther.* 22, 216 (2015).
42. S. A. K. Angarita *et al*., Human hepatocyte transplantation corrects the inherited metabolic liver disorder arginase deficiency in mice. *Mol. Genet. Metab.* **124**, 114–123 (2018).
43. E. K. Hsu *et al*., Analysis of liver offers to pediatric candidates on the transplant wait list. *Gastroenterology* **153**, 988–995 (2017).
44. C. Gustafsson, S. Govindarajan, J. Minshull, Codon bias and heterologous protein expression. *Trends Biotechnol.* **22**, 346–353 (2004).
45. D. An *et al*., Systemic messenger RNA therapy as a treatment for methylmalonic acidemia. *Cell Rep.* **21**, 3548–3558 (2017).
46. S. Khoja *et al*., Conditional disruption of hepatic carbamoyl phosphate synthetase 1 in mice results in hyperammonemia without orotic aciduria and can be corrected by liver-directed gene therapy. *Mol. Genet. Metab.* **124**, 243–253 (2018).
47. Q. Sun, W. E. O'Brien, Diagnosis of creatine metabolism disorders by determining creatine and guanidinoacetate in plasma and urine. *Methods Mol. Biol.* **603**, 175–185 (2010).
48. G. Allegri *et al*., A simple dried blood spot-method for in vivo measurement of ureagenesis by gas chromatography-mass spectrometry using stable isotopes. *Clin. Chim. Acta* **464**, 236–243 (2017).